

## **TENSION SOFTENING CURVES OF CONCRETE DETERMINED FROM DIFFERENT TEST SPECIMEN GEOMETRIES**

Y. Uchida,  
Department of Civil Engineering, Gifu University, Gifu, Japan  
B.I.G. Barr,  
Cardiff School of Engineering, University of Wales, Cardiff, UK

### **Abstract**

The main objective of this study was to investigate the dependency of tension softening curves of concrete upon the specimen geometry. For obtaining tension softening curves, three types of specimen geometry, i.e., beam, compact compression and compact tension, have been investigated. The tension softening curves of all three test geometries were determined by means of the poly-linear approximation analysis method. The analytical results show that the softening curves obtained from different specimens were almost identical.

Key words: Tension softening curve, fracture energy, test method

### **1 Introduction**

The most common specimen used for determination of fracture parameters of concrete is the notched beam subjected to three-point bending. A possible problem associated with the use of beam specimens is that the effect of the self-weight of the test specimen on the measured fracture parameters may be significant and should be considered. Additionally, it does not lend itself either to fabrication at a construction site or for use with cores drilled from existing concrete structures. To

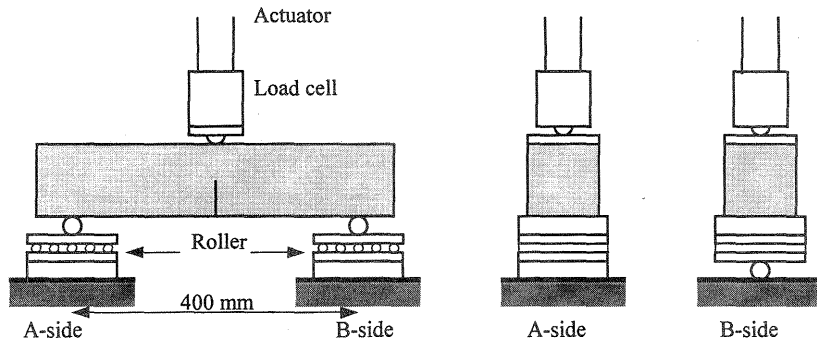
overcome these problems, alternative methods using compact specimens have been proposed. For example, the compact compression specimen was proposed by Barr et al. (1985) and the wedge splitting specimen was proposed by Bruhwiler et al. (1990). The principle of the wedge splitting specimen is the same as that for the compact tension specimen which is widely used for determining the fracture toughness of metallic materials. Basically, it has been considered that fracture parameters such as the fracture energy,  $G_F$ , are independent of the specimen geometry. However, there is little evidence in the literature regarding the dependency of tension softening curves of concrete upon the specimen geometry.

The main objective of this study was to investigate the dependency of tension softening curves of concrete upon the specimen geometry. Three kinds of geometries have been considered; beam, compact compression and compact tension. Three grades of concrete (40, 80 and 120MPa compressive strength) were used in the study in order to investigate a range of concrete response. The tension softening curves determined by means of the poly-linear approximation analysis method (PLAAM) proposed by Kitsutaka et al. (1994) were compared with the experimental results.

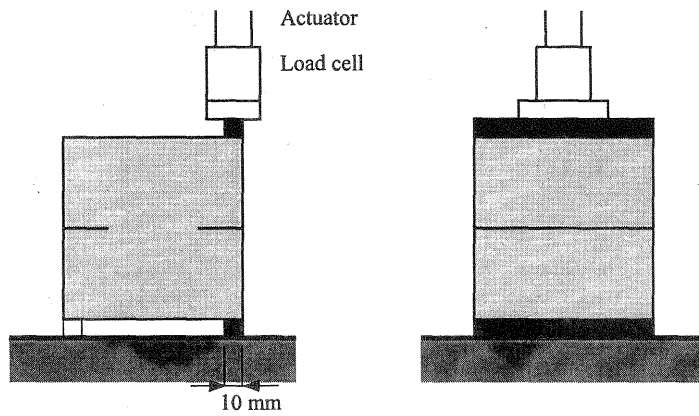
## 2 Experimental details

Three types of specimen geometries were investigated in this study, i.e., beam specimen, compact compression specimen and compact tension specimen. The beam specimen had dimensions of 100×100×500 mm and the notch depth and span length were 50 mm and 400 mm respectively as shown in Fig. 1(a). The compact compression specimen was prepared by notching 100 mm cube along two opposite faces as shown in Fig. 1(b). The notch depth ratio of the compact compression specimen was 0.25 for both notches. The compact tension specimen had dimensions of 200×200×100 mm with a notch length of 150 mm as shown in Fig. 1(c). Hence, all specimens had the same ligament size of 50×100 mm. For each test condition, the number of specimens was five.

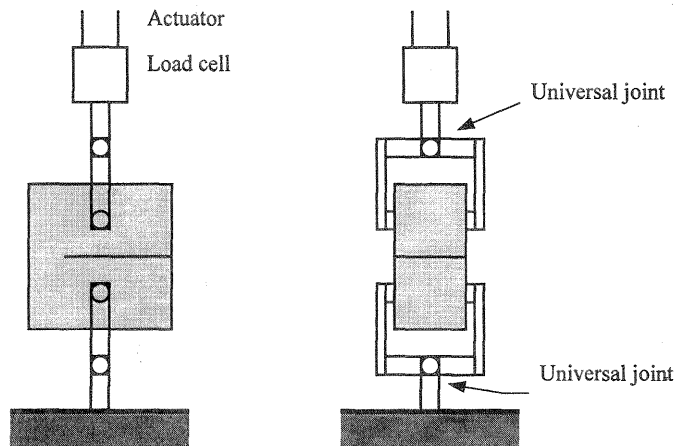
Three grades of concrete were tested in this study: nominal C40, C80 and C120. The mix proportions of the concrete are given in Table 1. The coarse aggregate was crushed limestone with a maximum size of 10 mm. For C80 and C120 concrete, microsilica in slurry form was used with a superplasticizer. All specimens were cured in water until immediately prior to testing. The notches were introduced by means of a masonry saw at the age of 3, 2 and 1 week for C40, C80 and C120, respectively. The concrete strength and Young's modulus, at the age of testing, are tabulated in Table 2.



(a) Beam in three-point bending ( $500 \times 100 \times 100$  mm prism)  
 (Notch depth / width: 50 mm / 2.5 mm)



(b) Compact compression ( $100$  mm cube) (Notch depth / width: 25-25 mm / 2.5mm)



(c) Compact tension ( $200 \times 200 \times 100$  mm prism) (Notch depth / width: 150 mm / 2.5mm)

Fig. 1. Test specimen geometries and loading arrangements

Table 1. Mix Proportions

Concrete Grade	C : S : A : W : SF*	W/C (W/B)	SP** (ml/kg × C)
C40	1.00 : 2.00 : 2.50 : 0.56 : -	0.56	-
C80	1.00 : 1.87 : 3.13 : 0.45 : 0.11	0.45 (0.41)	12.5
C120	1.00 : 1.32 : 2.21 : 0.24 : 0.11	0.24 (0.22)	45.0

\*SF: Silica fume, Solids , \*\*SP: Superplasticizer, Solution

Table 2. Strength and Young's modulus of concrete

Concrete Grade	Testing Age (days)	Compressive Strength* (MPa)	Tensile Strength** (MPa)	Young's Modulus** (GPa)
C40	34-42	48.2	4.46	39.7
C80	35-43	82.7	6.25	47.2
C120	38-44	117.4	7.69	47.8

\* 100mm cube specimen, \*\*  $\phi 100 \times 200$ mm cylindrical specimen

The loading configuration for each type of specimen is shown in Fig.1. The loading was carried out by a closed-loop hydraulic-controlled actuator with a maximum load capacity of  $\pm 20$  kN. During the loading test, load ( $P$ ), loading point displacement ( $LPD$ ) and crack mouth opening displacement ( $CMOD$ ) were measured. The  $LPD$  of the beam specimens was measured by an LVDT fixed to an aluminium yoke. The  $LPD$  of the compact compression/tension specimens was measured as the crack closing/opening displacement recorded by the clip gages, attached to the side of the specimen and in line with the loading points. The loading tests were carried out under crack mouth opening displacement control.

### 3 Determination of the tension softening curves

The tension softening curves of all three test geometries were determined by means of PLAAM. The details of PLAAM was reported by Uchida et al. (1995). The start point of the softening curve, i.e., tensile strength, has to be known in order to apply the PLAAM. The tensile strength can be estimated roughly as the transition point of the inclination of load-displacement curve or the splitting tensile strength of the concrete.

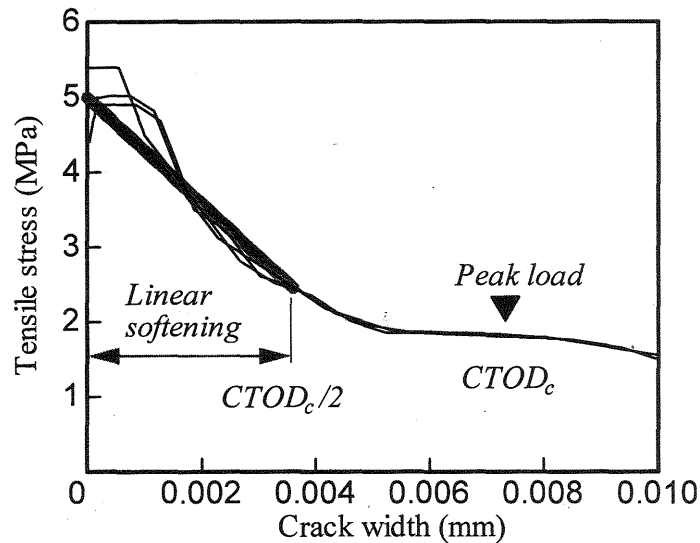


Fig. 2. Determination of tensile strength

However, it is almost impossible to determine the tensile strength as a unique value from the load-displacement curve, and the tensile strength of the softening curve is not identical with the tensile splitting strength.

Fig. 2 shows examples of the tension softening curves for the beam specimens (Grade C40 concrete) determined by means of the PLAAM with assumed different tensile strengths. The initial part of the softening curve depends on the assumed tensile strength. This means that it is impossible to determine a unique softening response by the curve fitting method. However, the softening curves where the crack width ( $\omega$ ) is larger than half the value of crack tip opening displacement at peak load ( $CTOD_c$ ) converge into a unique curve. Therefore, we adopted the following method to determine the unique softening curve. The softening curve where  $\omega > CTOD_c/2$  is determined as the mean curve obtained by the PLAAM assuming a minimum of three different appropriate tensile strengths. The region where  $\omega < CTOD_c/2$  is assumed to be a linear softening region and the tensile strength is optimized by minimizing the difference between the whole load-displacement curves obtained by experiment and analysis.

#### 4 Experimental results

The load - crack mouth opening displacement ( $P-CMOD$ ) curves and the load - load point displacement ( $P-LPD$ ) curves are shown in Figs 3

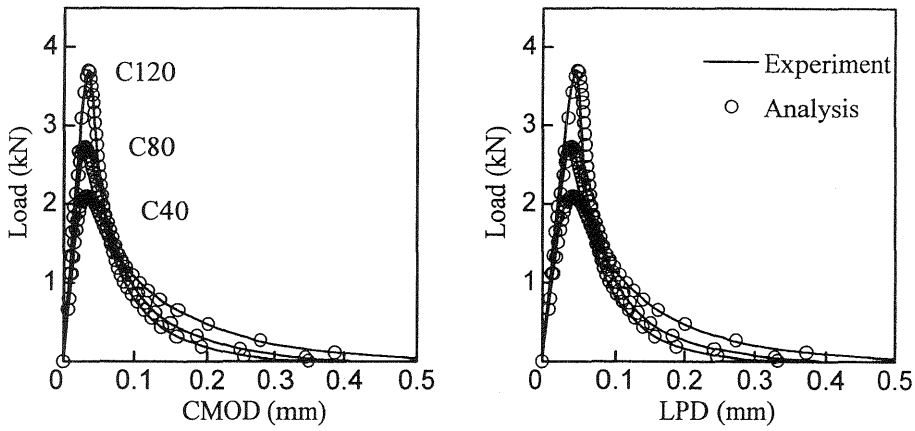


Fig. 3. Load-displacement curves for beam specimens

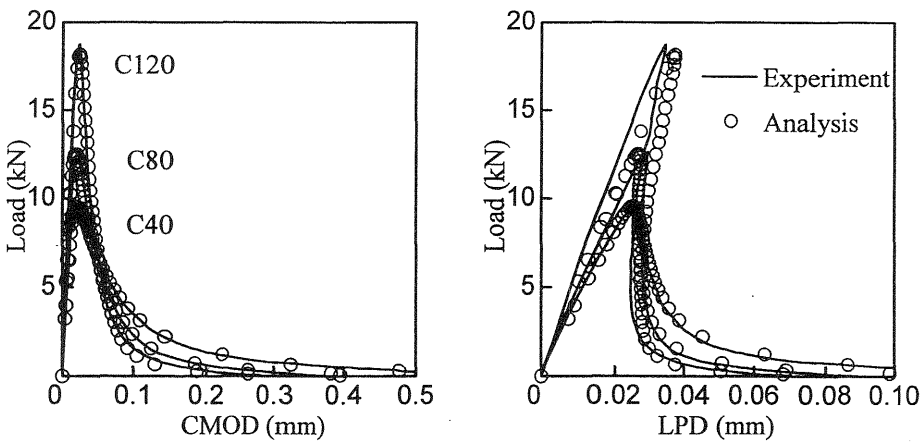


Fig. 4. Load-displacement curves for compact compression specimens

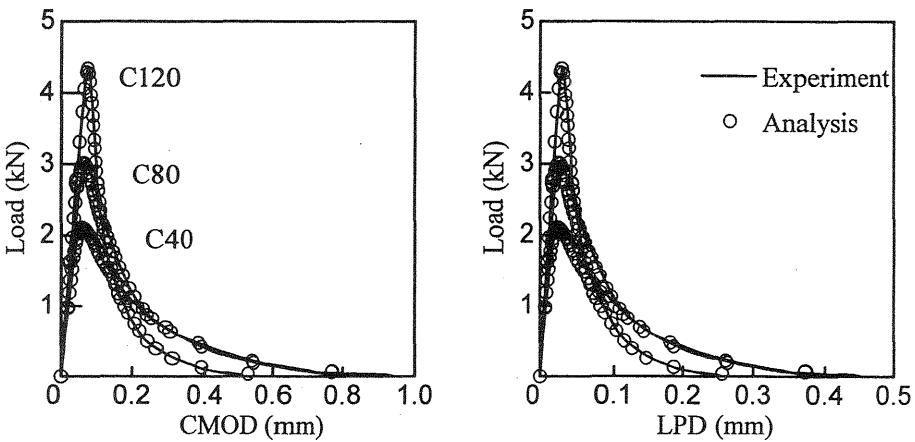


Fig. 5. Load-displacement curves for compact tension specimens

to 5. One of the five compact compression specimens for both C40 and C120 failed in shear adjacent to the loading line. From this result, 100 mm cube specimens with a notch depth ratio of 0.25 are considered as being on the limit for valid fracture tests. Snap-back phenomenon was observed for  $P-LPD$  curves for C80 and C120 compact compression specimens.

The work of fracture was measured as the area under the  $P-LPD$  curve. The fracture energy,  $G_F$ , was calculated according to the RILEM recommendations. The effect of the self-weight of the test specimens was considered for the beam specimens and the compact tension specimens, and ignored for the compact compression specimens. The results for  $G_F$  are given in Table 3 and illustrated graphically in Fig. 6.

The fracture energy determined indirectly from the  $P-CMOD$  curve,  $G_{F_{cmod}}$ , is also given in Table 3 and shown graphically in Fig. 6. To determine  $G_{F_{cmod}}$ , the final shape of the cracked specimens was assumed as two rigid half-specimens pivoting around a hinge located adjacent to the ligament edge remote from the crack tip. The position of this virtual hinge was assumed to be identical for all specimens, and has been estimated as the position which results in the difference between  $G_F$  and  $G_{F_{cmod}}$  being a minimum. Using this assumption, the depth of the hinge was estimated at 2.5 mm for the results obtained in this study. The  $G_{F_{cmod}}$ , with a hinge depth of 2.5 mm, shows good correspondence with

Table 3 Test results

Specimen*	$P_{max}$ (kN)	$CMOD_u$ (mm)	$LPD_u$ (mm)	$G_F$ (N/m)	$G_{F_{cmod}}$ (N/m)
BM-C40	2.12	0.653	0.628	67.7	65.5
BM-C80	2.80	0.409	0.393	57.6	55.1
BM-C120	3.73	0.353	0.340	53.8	51.6
CC-C40	9.62	0.600	0.136	58.1	52.2
CC-C80	12.83	0.373	0.089	46.6	40.8
CC-C120	18.85	0.282	0.070	48.0	40.8
CT-C40	2.16	0.940	0.451	60.8	60.9
CT-C80	3.06	0.904	0.447	68.9	68.4
CT-C120	4.39	0.515	0.253	53.7	54.2

\* BM: Beam, CC: Compact compression, CT: Compact tension  
C(40 80 120): Concrete grade

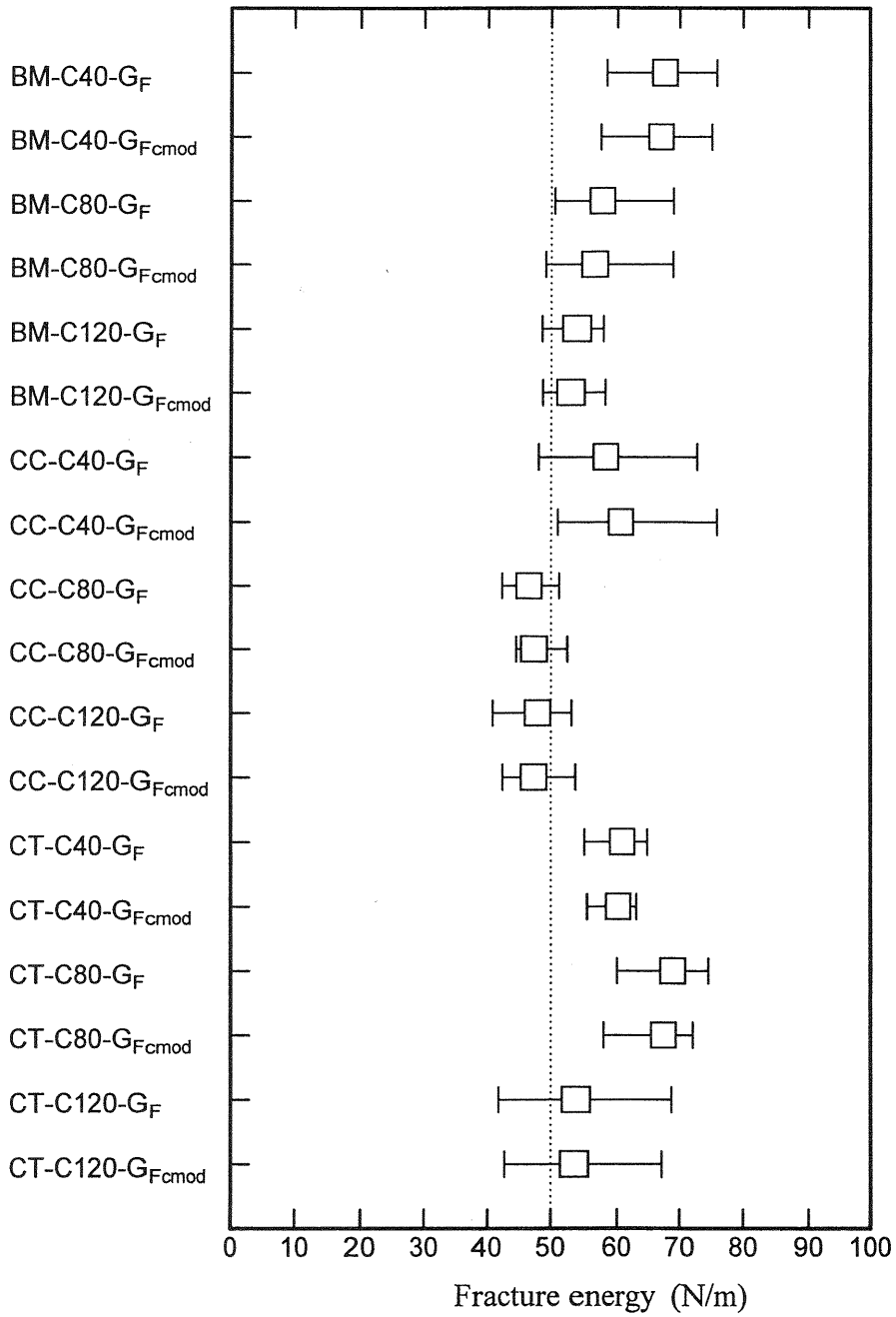


Fig. 6. Summary of fracture energy results

$G_F$  results as shown in Fig. 6. This result suggests that the fracture energy  $G_F$  can be determined indirectly from the  $P-CMOD$  curve. However, it should be noted that the depth of the hinge would be affected by variations in the concrete such as different maximum aggregate size, etc. and also possibly by the size of the specimen.

Much of the evidence in the literature suggests that  $G_F$  values increase as the strength of concrete increases. On the contrary,  $G_F$  values in this study were constant or decreased with increasing strength. One of the reasons for this result is considered to be that the bridging effect of the aggregates becomes weaker as the strength increases because the crack surface becomes plane as the strength of the mortar matrix becomes higher. Observation by naked eye after the loading tests showed that the fracture surfaces of the specimens were more plane as the strength of concrete increased. Furthermore, the final values of displacements ( $CMOD_u$  and  $LPD_u$  in Table 3) decreased as the strength increased as given in Table 3.

The  $G_F$  values from the beam specimens and the compact tension specimens were almost identical. On the other hand, the  $G_F$  values from the compact compression specimens had a tendency to be smaller than the corresponding values from beam specimens and the compact tension specimens.

## 5 Analytical results

The softening curves, determined through the PLAAM, are presented in Figs. 7 to 9. There are slight differences among the softening curves obtained from different specimens, but it is seen that the softening curve is basically independent of the specimen geometry.

Fig. 10 shows the non-dimensional softening curves for beam specimens with different concrete grades. The shape of the softening curves for C40 and C80 seem to be modeled by the bi-linear function, whereas the softening curve of C120 seems to be almost linear.

Table 4 shows a comparison between the tensile strength determined in the analysis and that obtained in split cylinder test. In all cases, the experimental splitting tensile strength was lower than the corresponding values in the analysis and the difference increased as the strength of concrete increased. In this study, the tensile strength determined in the analysis is about one tenth of the cube compressive strength.

The  $P-CMOD$  and the  $P-LPD$  curves were simulated through the FE-analysis with the numerical softening curves and are plotted in Fig.3 to 5. All of the simulated curves agree well with the experimental curves and the snap-back phenomenon of  $P-LPD$  relationships for compact compression specimens of grade C80 and C120 concrete are also

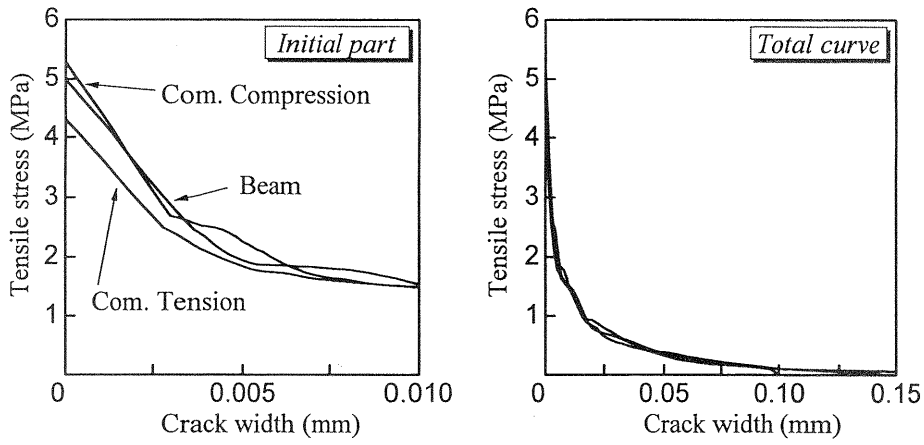


Fig. 7 Tension softening curves for C40

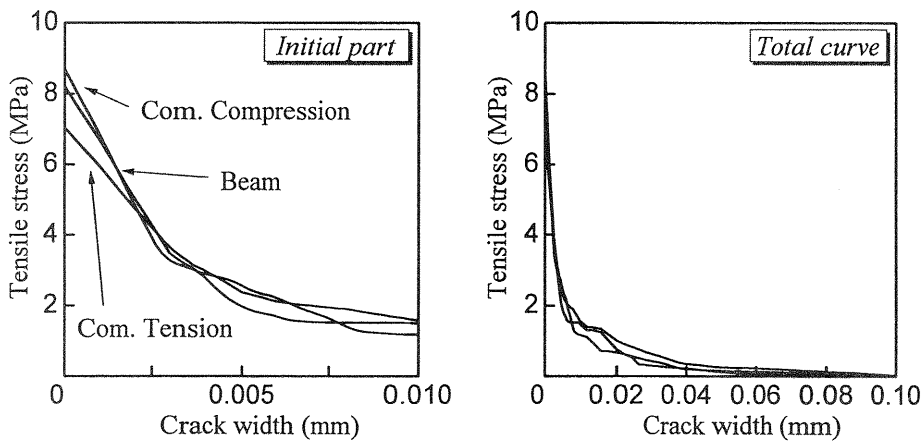


Fig. 8 Tension softening curves for C80

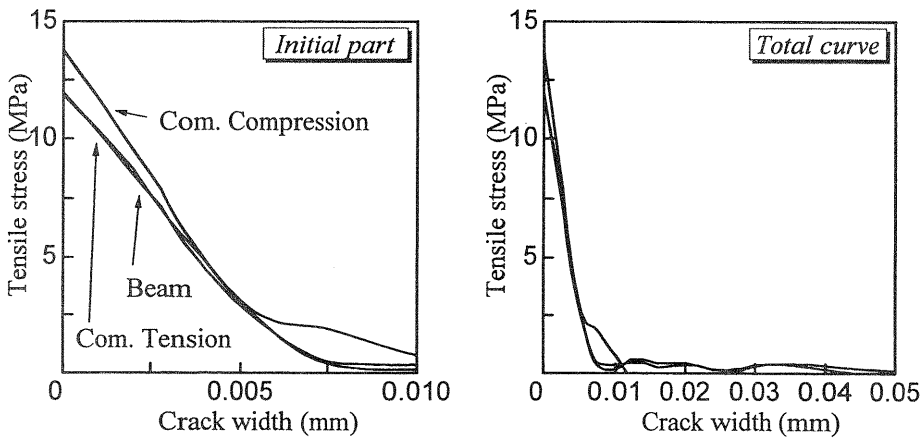


Fig. 9 Tension softening curves for C120

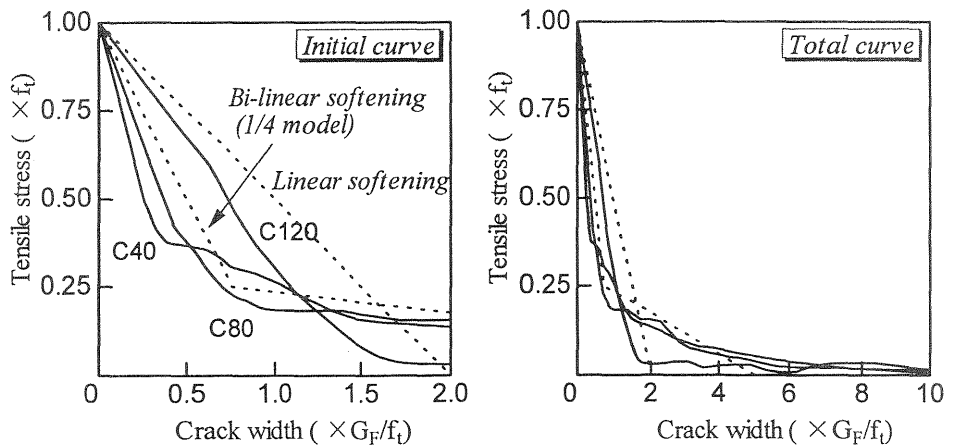


Fig. 10. Non-dimensional tension softening curves for beam specimens

Table 4 Tensile Strength

Concrete Grade	Specimen	Tensile strength from analysis (MPa)	Concrete strength (MPa)	
			Split Tens.	Comp.
C40	Beam	5.0	4.46	48.2
	C.Comp.	5.3		
	C.Tens.	4.3		
C80	Beam	8.2	6.25	82.7
	C.Comp.100	8.7		
	C.Tens.	7.1		
C120	Beam	12.0	7.69	117.4
	C.Comp.	13.7		
	C.Tens.	11.9		

simulated with good accuracy. From these results, it is considered that PLAAM is a very effective method for the determination of softening curves of concrete.

## 6 Conclusions

Three types of specimen geometry and three grades of concrete for obtaining tension softening curves have been investigated. In the

experimental study, valid fracture energy,  $G_F$ , results can be determined via  $P-CMOD$  curves which are significantly easier to obtain experimentally than the  $P-LDP$  curves. The  $G_F$  values from the beam specimens and the compact tension specimens were almost identical. On the other hand, the  $G_F$  values from the compact compression specimens were marginally lower than the corresponding results from the other two specimens.

In the analytical study, the tension softening curves of all three test geometries were determined by means of the PLAAM. The softening curves obtained from different specimens were almost identical. The load-displacement curves simulated through the FE-analysis using the numerical softening curves agreed well with the experimental curves.

### Acknowledgments

The first author wishes to express his gratitude for the financial support of the Japan Society for the Promotion of Science to visit to the University of Wales Cardiff, during which time this study was carried out.

### References

- Barr, B.I.G, and Sabir, B.B. (1985) Fracture toughness testing by means of the compact compression test specimen. **Magazine of Concrete Research**, 37, 88-94.
- Brühwiler, E. and Wittmann, F.H. (1990) The wedge splitting test - a method of performing stable fracture mechanics tests, in **Fracture and Damage of Concrete and Rock** (ed. H.P. Rossmanith), Pergamon Press, Oxford, 117-126.
- Kitsutaka, Y., Kamimura, K. and Nakamura (1994) Evaluation of aggregate properties behavior on tension softening behavior of high strength concrete, **High Performance Concrete**, ACI SP149-40, 711-727.
- Uchida, Y., Rokugo, K. and Koyanagi, W. (1995) Determination of tension softening diagrams of various kinds of concrete by means of numerical analysis. in **Fracture Mechanics of Concrete Structures**, Proceedings FRAMCOS-2 (ed. F.H. Wittmann), AEDIFICATIO Publishers, D-79104 Freiburg, 17-30.